Biotechnol Lett (2020) 42:2211–2221
https://doi.org/10.1007/s10529-020-02928-8

ORIGINAL RESEARCH PAPER

Improving the thermostability of a GH97 dextran glucosidase by rational design

Xiaomin Zhang · Feiyun Chen · Chao He · Wei Fang · Zemin Fang · Xuecheng Zhang · Xiaotang Wang · Yazhong Xiao

Received: 11 December 2019 / Accepted: 29 May 2020 / Published online: 1 June 2020

Abstract This study was aimed at improving the thermostability of dextran glucosidase PspAG97A, a member of the glycoside hydrolase family 97, from *Pseudoalteromonas* sp. K8. A total of 9 lysine residues were chosen using the TKSA-MC program based on the optimization of surface charge-charge interactions and were mutated to glutamate for shifting the enzyme's isoelectric point off its optimum pH value. Three mutants K75E, K363E and K420E showed enhanced thermostability. The triple mutant, K75E/K363E/K420E, was found to be the best with a 7.3-fold increase in half-life ($t_{1/2}$) at 33 °C compared to that of the wild-type (WT). Most importantly, this mutant showed comparable enzymatic activity to that of the WT protein. Structural modelling demonstrated that increased surface charge-charge interactions and optimization of surface hydrophobic and electrostatic contacts contributed to the improved thermostability displayed by K75E/K363E/K420E.

Keywords Dextran glucosidase · GH97 · Surface charge–charge interactions · Isoelectric point · Thermostability improving · Structural modelling

Introduction

Microbial dextran is a homoglycan of α-D-glucopyranose molecule connected primarily by α-1,6 linkages, with various extents of branches via -1,2, -1,3, or -1,4 linkages to the main chain. Dextranases hydrolyze dextran to oligosaccharides and are widely used in pharmaceutical, sugar, and dental industries (Khalikova et al. 2005). In sugar industry, dextranase is used to reduce the viscosity and to increase sucrose recovery of juices (Jiménez 2009). In pharmaceutical industry, dextranase can be used with commercial dextran to produce low molecular weight clinical grade dextran as plasma substitutes (Wu et al. 2011) or isomaltooligosaccharides as prebiotics (Gan et al. 2014; Goulas et al. 2004). In dental industry,

Electronic supplementary material The online version of this article (https://doi.org/10.1007/s10529-020-02928-8) contains supplementary material, which is available to authorized users.

X. Zhang · F. Chen · C. He (✉) · W. Fang · Z. Fang · X. Zhang · Y. Xiao (✉)
School of Life Sciences, Anhui University, Hefei 230601, Anhui, China
e-mail: chaohe@ahu.edu.cn

Y. Xiao
e-mail: yzxiao@ahu.edu.cn

X. Zhang · F. Chen · C. He · W. Fang · Z. Fang · X. Zhang · Y. Xiao
Anhui Key Laboratory of Modern Biomanufacturing, Hefei 230601, Anhui, China

X. Wang
Department of Chemistry and Biochemistry, Florida International University, Miami, FL 33199, USA

dextranase is added to oral care products, such as toothpaste and mouthwash, for degrading dextran in dental plaques and dislodging biofilm produced by *Streptococcus mutans*, a primary pathogen of dental caries (Pleszczynska et al. 2017).

Dextranases are classified into two broad categories, endo- and exo-dextranases, depending on their action patterns on dextran. Three types of exo-dextranases have been reported, glucodextranase (also referred to as dextran glucosidase, EC 3.2.1.70) (Linder and Sund 1981; Mizuno et al. 2004; Morimoto et al. 2004; Saburi et al. 2015; Takahashi 1982), isomalto-dextranase (EC 3.2.1.94) (Okazawa et al. 2015) and isomaltotrio-dextranase (EC 3.2.1.95) (Mizuno et al. 1999). These exo-dextranases hydrolyze dextran from the non-reducing end to produce glucose, isomaltose and isomaltotriose, respectively. We have expressed and characterized an α-glucoside hydrolase, PspAG97A, produced by the deep-sea bacterium *Pseudoalteromonas* sp. K8 (Li et al. 2016). PspAG97A represents the first reported glucodextranase from marine bacteria that belongs to glycoside hydrolase GH97 family with high catalytic efficiency for dextran and unique features, like alkaline-adaption, moderate-temperature catalysis and halophilic. When *p*-nitrophenyl α-D-glucopyranoside was used as substrate, PspAG97A showed the highest activity at pH 7.5 and 30 °C in 0.8–1 M NaCl. Dextranases working efficiently under both alkaline and moderate-temperature conditions have been seldomly reported (Khalikova et al. 2005). PspAG97A from marine microorganism was an exception and may have application potential in dental products since alkaline oral care products are more protective to enamel than acidic products (Majeed et al. 2011). However, the relative instability and moderate rate of inactivation (maintaining only 50% of its activity after incubation at 30 °C for 7 h) severely limits the industrial applications of PspAG97A.

The crystal structure of PspAG97A (He et al. 2016) makes it possible to improve the thermostability of this unique dextranase by rational design. PspAG97A possesses an isoelectric point (pI) of 7.33, propinquant to the enzyme's optimum pH of 7.5. The close proximity of the enzyme's pI to its optimum pH generally prevents the application of the protein at optimum condition due to protein aggregation and instability. On the other hand, Makhatadze et al. has explored the optimization of the energy of the charge-charge interactions on protein surface via the Tanford–Kirkwood solvent accessibility (TKSA) model (Makhatadze 2017). Based on this model, optimization of charge-charge interactions via directed mutations has successfully enhanced the thermal stability of many different proteins (Gribenko et al. 2009; Tu et al. 2015). However, this strategy has not been applied to a dextran glucosidase. Therefore, we have constructed several mutants of PspAG97A using a free web server that calculates protein charge-charge interactions via the TKSA model with the Monte Carlo sampling method (Contessoto et al. 2018). All three single point mutants, K75E, K363E and K420E, showed enhanced thermostability. The triple mutant, K75E/K363E/K420E, was found to be the best with a 7.3-fold increase in half-life ($t_{1/2}$) at 33 °C and essentially identical activity compared to that of the WT protein. This work demonstrates the successful application of rational design guided by the TKSA-MC model in improving the stability and activity of target proteins.

Materials and methods

Selection of mutation sites and site-directed mutagenesis

Charge-charge interaction energy ΔGqq for each ionizable residue was calculated by the TKSA-MC model (Contessoto et al. 2018) with input file of PDB ID: 5HQ4 and input parameters of pH 7.5 and temperature 308 K. The recombinant plasmid with the wild-type PspAG97A gene (residues 20–680, without the predicted *N*-terminal signal peptide), pET-28a-*pspag97a*, was used as the template. Site-directed mutagenesis was conducted using the Site Directed Mutagenesis Kit (TaKaRa) according to the manufacturer's instructions. Once the sequence of the mutant enzyme gene was confirmed by sequencing, the expression plasmids were transformed into *E. coli* BL21 (DE3).

Protein expression and purification

The transformant was cultured in LB medium at 37 °C until OD_{600} reached about 0.8. Protein expression was induced with 0.1 mM isopropyl β-D-1-thiogalactopyranoside (IPTG) at 16 °C for 24 h. The cell pellet was

collected by centrifugation of the culture media at 4000 rpm for 10 min and resuspended and disrupted in buffer A (20 mM Tris–HCl, pH 8.5, 500 mM NaCl). After centrifugation, the supernatant was loaded onto a HisTrap nickel-Sepharose column (GE Healthcare), and the protein was eluted with buffer A containing a step gradient of 50–250 mM imidazole. The purified protein was then concentrated for subsequent analysis. Protein purity was examined by SDS-PAGE and protein concentration was determined by the Bradford protein assay using bovine serum albumin as the standard.

Dextran substrate specificity

For substrate specificity of PspAG97A, we investigated the activities by using 5% (*w/v*) commercial dextrans T5, T10, T20, T40 and T70 (obtained from Shanghai Aladdin Bio-Chem Technology Co., LTD) in buffer B (50 mM Na_2HPO_4–KH_2PO_4, pH 7.5, 800 mM NaCl). After incubation at 35 °C for 5 min, the reaction was quenched with boiling water and centrifugation. The amount of glucose released was colorimetrically determined using the Glucose Assay kit (Shanghai Rongsheng Biological Pharmaceutical Co., Ltd.) at 505 nm. Glucose was used as the standard. One unit of activity was defined as the amount of enzyme required to liberate 1 μmol of glucose per minute at 35 °C and pH 7.5. Relative activity was expressed as percentage of the highest activity (100%) toward T5. All assays were conducted in triplicate.

Effects of temperature on activity and stability of enzymes

The optimal temperature of the enzymes was determined by measuring the enzyme activity at different temperatures (10–50 °C) in buffer B, using 5% (*w/v*) T5 as substrate. Relative activity was expressed as percentage of the highest activity (100%). All assays were conducted in triplicate. To assess thermal stability, the enzyme solution was pre-heated at 35 °C or 33 °C for different times and rapidly cooled. The residual activity was measured using the assay described above.

Effects of pH on enzyme activity

To determine the optimal pH of the enzymes, activity was measured in buffers of different pH containing 800 mM NaCl and 5% (*w/v*) dextran T5 at 35 °C. Solutions with different pH values were used as follows: 50 mM Na_2HPO_4-KH_2PO_4 buffer (pH 6.0–7.0) and 50 mM Tris–HCl buffer (pH 7.0–9.0). Relative activity was expressed as percentage of the highest activity (100%). All trials were conducted in triplicate.

Products of enzyme hydrolysis

Recombinant WT PspAG97A and K75E/K363E/K420E mutant catalyzed hydrolysis of 5% (*w/v*) dextran T5 took place at 35 °C in buffer B. For TLC analysis, reaction products were developed twice on a silica gel plate (Haiyang Chemical Co., Ltd, Qingdao, China) with a mobile phase consisting of trichloromethane/acetic acid/water (4:9:1 by volume) and then visualized using sulfuric acid/ethanol (1:9 by volume), followed by heating the plate at 80 °C for 5 min.

Determination of kinetic parameters

Kinetic parameters of purified WT PspAG97A and its mutant enzymes were determined with 5% (w/v) dextran T5 at 35 °C in buffer B. The initial velocity was determined by plotting absorbance versus time for each substrate concentration. The k_{cat}, K_m, and k_{cat}/K_m were calculated by fitting the data to the Michaelis–Menten equation using nonlinear regression with Origin.

Structural analysis

The structural model of the K75E/K363E/K420E mutant was generated on the basis of the PspAG97A structure (PDB ID: 5HQ4) by Modeller 9.16 (Webb and Sali 2016). The PyMol Molecular Graphics System (DeLano Scientific LLC, San Carlos, CA, USA) was used for the visualization and analysis of the protein structure.

Circular dichroism (CD)

Far-UV CD spectra were recorded at 25 °C with circular dichroism spectrometer (Applied Photophysics) between 180 and 260 nm using a 1 mm path length cell and approximately 500 µg/ml protein sample in buffer B. A buffer only reference was subtracted from each curve.

Fluorescence spectroscopy

Intrinsic fluorescence measurements of the proteins were recorded at 25 °C with a Shimadzu RF 5301 spectrofluorophotometer in a 0.1 cm path length quartz cell using approximately 200 µg/mL protein sample in buffer B. Fluorescence emission spectra were recorded from 300 to 450 nm using an excitation wavelength of 280 nm.

Results

PspAG97A hydrolyzes various molecular weight dextrans

The activities of PspAG97A in the catalyzed hydrolysis of dextrans of different molecular weights were determined. PspAG97A showed the highest activity at 35 °C and pH 7.5 with dextran T5, which has an average molecular weight of 5 kDa (Table 1). As the molecular weight of the dextran substrate increased, the specific activity of the enzyme decreased gradually. The highest specific activity toward 5% (*w*/*v*) T5 was about 1086 U/mg. When the specific activity toward T5 was taken as 100%, this enzyme displayed about 97.1%, 77.75%, 67.15% and 62.3% relative activities toward 5% (*w*/*v*) T10, T20, T40 and T70 with average molecular weights of 10, 20, 40 and 70 kDa, respectively. These results showed that PspAG97A can hydrolyze dextrans of various molecular weights with the highest activity toward 5% (*w*/*v*) T5, the substrate used in the following activity and thermostability assays.

Table 1 Dextran substrate specificity of PspAG97A

Substrate	Specific activity (U/mg)	Relative activity (%)
Dextran T5	1085.84 ± 50.40	100
Dextran T10	1054.35 ± 4.11	97.10
Dextran T20	844.19 ± 39.04	77.75
Dextran T40	729.19 ± 7.21	67.15
Dextran T70	676.48 ± 11.43	62.30

Choice of residues for site-directed mutagenesis

Lysine residues are the most abundant among all positively charged residues present on the surface of PspAG97A. Compared to arginine residues, lysine residues participate less often in multipoint electrostatic interactions. Thus, it was decided to decrease the isoelectric point by substituting lysine residues on the surface of the protein. The TKSA-MC analysis (Contessoto et al. 2018) allows the calculation of the charge-charge interaction free energy (ΔGqq, Fig. 1a) of each ionizable residue. The bars indicate the ΔGqq contribution of each ionizable residue to the stability

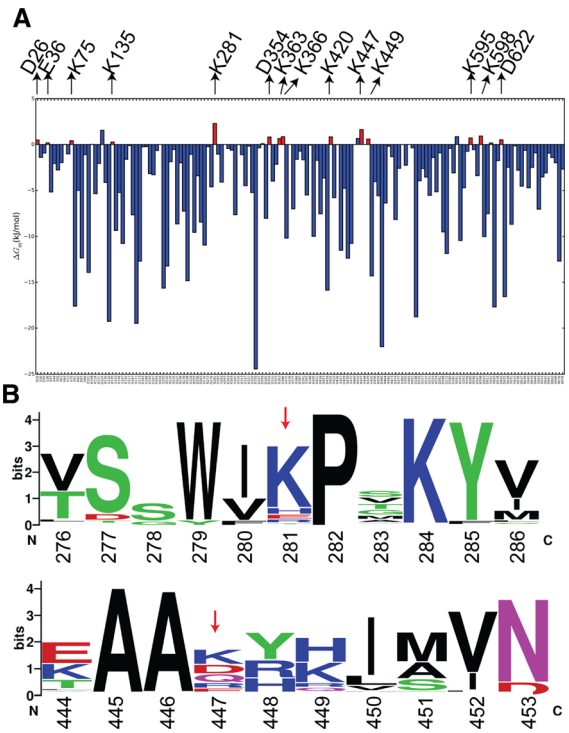

Fig. 1 **a** Charge-charge interaction energy, ΔGqq, calculated by the TKSA-MC model for each ionizable residue of PspAG97A. The simulation parameters were pH 7.5 and 308 K. The PspAG97A structure used was PDB ID: 5HQC. **b** Multiple sequence alignment of GH97 inverting subfamily members from the CAZy database

of protein's native state when compared to the unfolded state. The red bars indicate the candidate residues to be mutated to increase protein stability. For PspAG97A at the optimal condition (pH 7.5 and 35 °C), the highlighted fourteen residues are D26, E36, K75, K135, K281, D354, K363, K366, K420, K447, K449, K595, K598, D622, eleven of which are lysine (Fig. 1a). Moreover, the candidate for lysine substitution should not be conserved. Multiple sequence alignment revealed that K281 and K447 are relatively conserved in GH97 inverting subfamily (Fig. 1b). Based on the above analysis, nine lysine residues at positions 75, 135, 281, 363, 366, 420, 449, 595 and 598 were chosen as targets for introducing mutations. As K281 presents the highest unfavorable ΔGqq, it was also included as a target despite being conservative. The negatively charged glutamate was chosen to replace the positively charged lysine residue(s) to achieve the expected dramatic reduction in the enzyme's pI value.

Thermostability assays of WT and the nine single point mutants

The genes encoding the WT and mutant enzymes were cloned and expressed in *E. coli* BL21(DE3). After purification by Ni-affinity chromatography, each of the mutant proteins migrated as a single band and displayed the same molecular weight as WT on SDS-PAGE (Supplementary Fig. 1). PspAG97A showed poor thermostability at its optimum temperature of 35 °C, with only 57.8% activity retained after

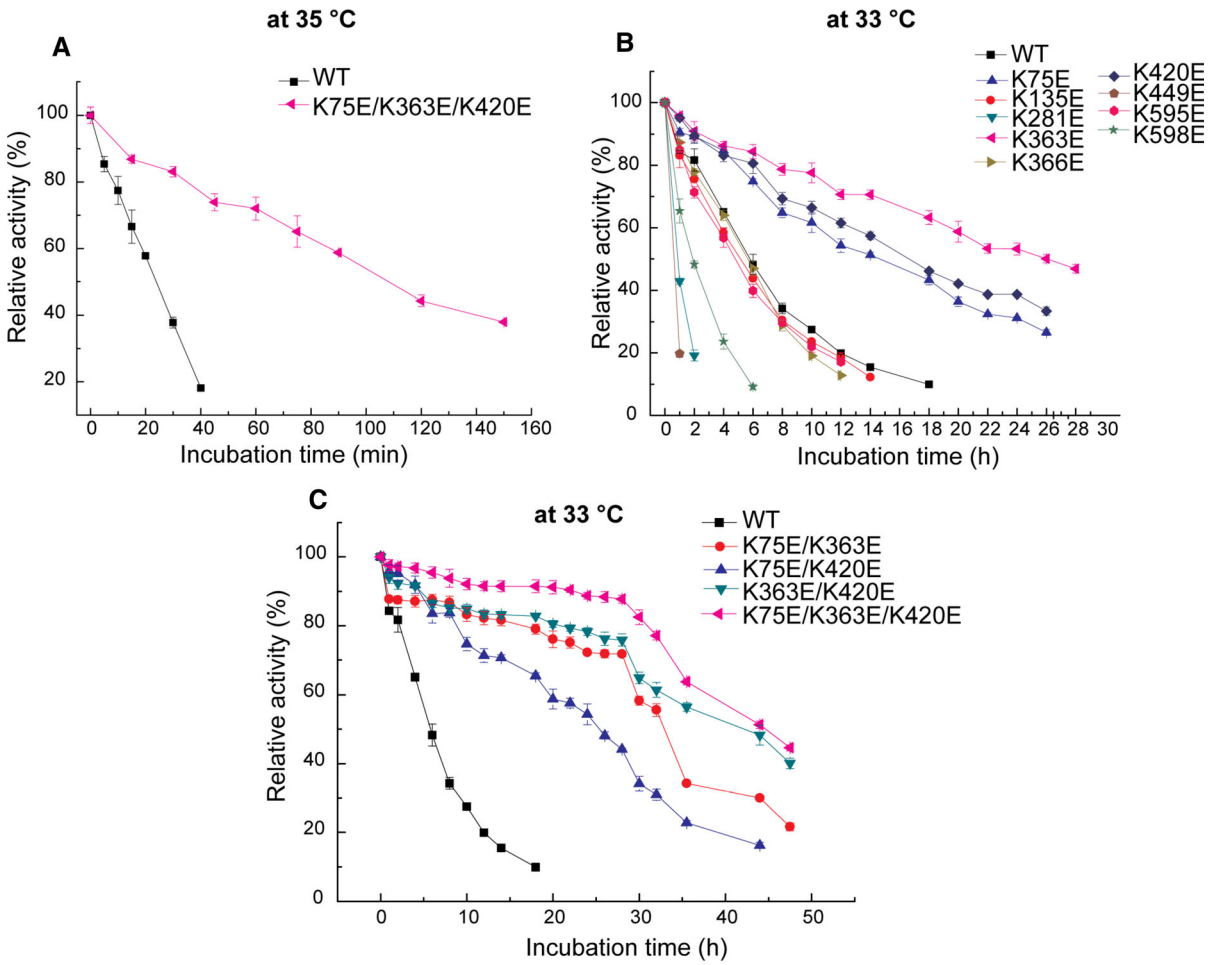

Fig. 2 **a** Thermostability of WT PspAG97A and its K75E/K363E/K420E triple mutant at 35 °C. **b** Thermostability of WT PspAG97A and its nine single point mutants at 33 °C. **c** Thermostability of PspAG97A and its four combinational mutants at 33 °C

Table 2 Characteristics of WT PspAG97A and its mutants with dextran T5 as substrate

Enzyme	[a]T_{opt} (°C)	[b]pH_{opt}	[c]$t_{1/2}$ at 33 °C (h)
WT	35	7.5–8.0	6
K75E	35	7.5–8.0	14
K135E	35	7.5–8.0	5
K281E	35	7.5–8.0	< 1
K363E	35	7.5–8.0	26
K366E	35	7.5–8.0	6
K420E	35	7.5–8.0	17
K449E	35	7.5–8.0	< 1
K595E	35	7.5–8.0	4
K598E	35	7.5–8.0	2
K75E/K420E	40	7.0–7.5	24
K75E/K363E	40	7.0–7.5	32
K363E/K420E	40	7.0–7.5	36
K75E/K363E/K420E	40	7.0–7.5	44

[a]T_{opt}, optimum temperature

[b]pH_{opt}, optimum pH

[c]$t_{1/2}$, half-life value

incubation for 20 min (Fig. 2a). We then selected a lower temperature 33 °C to determine the thermostability of the WT and mutant enzymes. As shown in Table 2 and Fig. 2b, the $t_{1/2}$ values at 33 °C for the K363E, K420E and K75E mutants were about 26 h, 17 h and 14 h, respectively, higher than that for the WT (only 6 h). The other six mutants, K135E, K281E, K366E, K449E, K595E and K598E, showed similar or lower $t_{1/2}$ values than that for the WT. In addition, the three thermostability-enhanced single point mutants had similar optimum temperature and pH (35 °C and pH 7.5–8.0) (Table 2), all retaining more than 80% activity within the ranges of 35–40 °C and pH 7.0–8.0 (Supplementary Fig. 2).

Construction of double and triple mutants and their thermostability assays

To further improve the thermostability of PspAG97A, we performed multiple mutations by constructing three double mutants K75E/K363E, K75E/K420E and K363E/K420E, and one triple mutant K75E/K363E/K420E. The theoretical pI value was reduced from 7.33 to 6.44 for the triple mutant K75E/K363E/K420E. All mutants had good protein purity (Supplementary Fig. 3). As shown in Table 2 and Fig. 2c, the $t_{1/2}$ values at 33 °C for K75E/K420E, K75E/K363E, K363E/K420E and K75E/K363E/K420E mutants were 24, 32, 36 and 44 h, respectively, significantly higher than that of the WT protein. The triple mutant also showed improved thermostability at 35 °C with 58.8% activity retained after 90 min incubation (Fig. 2a). In addition, the four combinational mutants had similar optimum temperature and pH (40 °C and pH 7.0–7.5) (Table 2), all retaining more than 80% activity within the ranges of 35–40 °C and pH 7.0–8.0 (Supplementary Fig. 4). These results demonstrated that the triple mutant K75E/K363E/K420E was the best in terms of improving the thermostability of PspAG97A.

Kinetic parameters and hydrolysis products of WT and the mutants

The kinetic parameters of the WT and thermostability-enhanced mutants were determined at 35 °C and pH 7.5 using ten different substrate concentrations of dextran T5. As shown in Table 3, the K_m, k_{cat} and k_{cat}/

Table 3 The kinetic parameters of WT PspAG97A and its mutants at 35 °C and pH 7.5 with 5% (*w*/*v*) dextran T5 as substrate

Name	V_{max} (μmol mg^{-1} min^{-1})	K_m (mM)	K_{cat} (s^{-1})	K_{cat}/K_m (s^{-1} mM^{-1})
PspAG97A	1217.48 ± 19.31	1.12 ± 0.08	0.0192	17.14
K75E	1224.76 ± 15.60	1.18 ± 0.07	0.0193	16.40
K363E	1163.95 ± 20.53	1.04 ± 0.09	0.0183	17.60
K420E	1268.14 ± 40.78	1.28 ± 0.17	0.0200	15.63
K75E/K363E	1371.07 ± 21.62	0.91 ± 0.07	0.0216	23.74
K75E/K420E	1363.49 ± 19.14	0.93 ± 0.06	0.0215	23.12
K363E/K420E	1306.90 ± 24.41	0.95 ± 0.09	0.0206	21.68
K75E/K363E/K420E	1381.43 ± 28.08	1.00 ± 0.10	0.0218	21.80

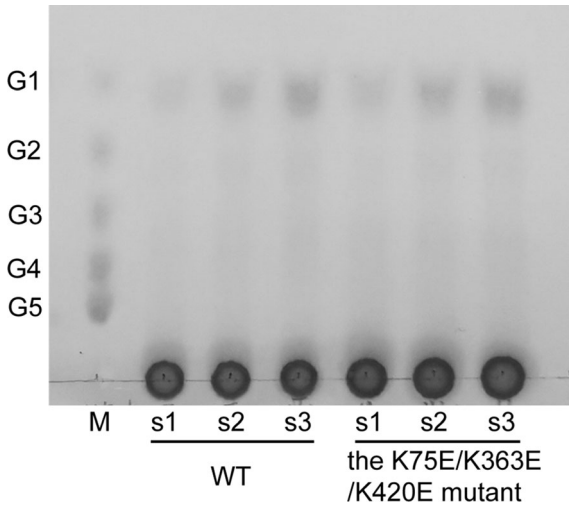

Fig. 3 Thin-layer chromatogram of the products from WT PspAG97A and its triple mutant, K75E/K363E/K420E. Symbols: G1–G5 a series of authentic sugar standards of glucose, maltose, maltotriose, maltotetrose, and maltopentaose, respectively. M is the standard marker, s1–s3 show the 10 min, 20 min, and 30 min reaction times for WT PspAG97A and K75E/K363E/K420E, respectively

K_m values of these mutants were almost similar to that of WT, suggesting that although these mutations improved the thermostability of PspAG97A, they did not affect the binding affinity between protein and substrate, the turn-over number, and the catalytic efficiency of the enzyme. Moreover, the hydrolysis products catalyzed by WT and the best performing mutant K75E/K363E/K420E were analyzed through TLC with 5% dextran T5 as substrate at 35 °C and pH 7.5 for different periods (10 min, 20 min and 30 min). As the reaction progressed, the amount of glucose produced increased (Fig. 3), confirming that both PspAG97A WT and its best performing mutant are glucose-forming exodextranases.

Structural modelling and explanation for the improved thermostability

To explain why thermostability was enhanced for these mutants, the overall structures of the thermostability-enhanced mutants were compared with that of the WT protein. The CD spectra of these mutants and WT were similar (Fig. 4a), indicating no significant secondary structural changes were induced by the mutations. In addition, fluorescence spectra showed that these mutants and WT exhibited the maximum emission at the same wavelength of 340 nm (Fig. 4b), suggesting that the overall tertiary structures of these mutants remained similar as that of the WT. Structural modelling of the mutant K75E/K363E/K420E was then performed. According to the model, the hydrophobic and electrostatic interactions between residue-75 and its surrounding residues Gln77 and Thr74 are likely optimized for the K75E mutation (Fig. 5a, b). Additional electrostatic interactions might be formed between E363 and K366 (Fig. 5c, d), and between E420 and R417 (Fig. 5e, f). Therefore, we postulated that additional charge-charge interactions and optimization of surface hydrophobic and electrostatic contact resulted in the improved thermostability of the K75E/K363E/K420E mutant.

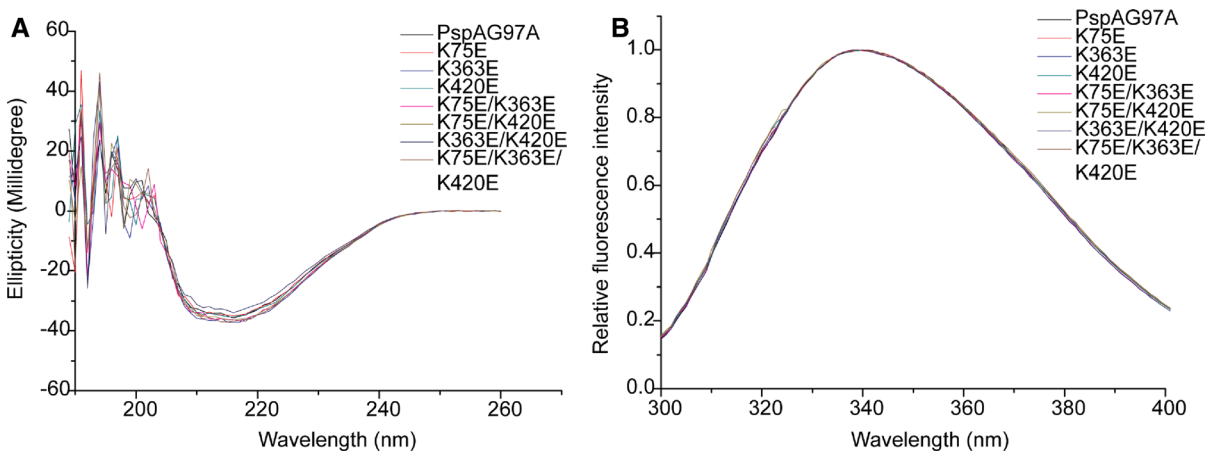

Fig. 4 The CD (**a**) and intrinsic fluorescence (**b**) spectra of WT PspAG97A and its mutants

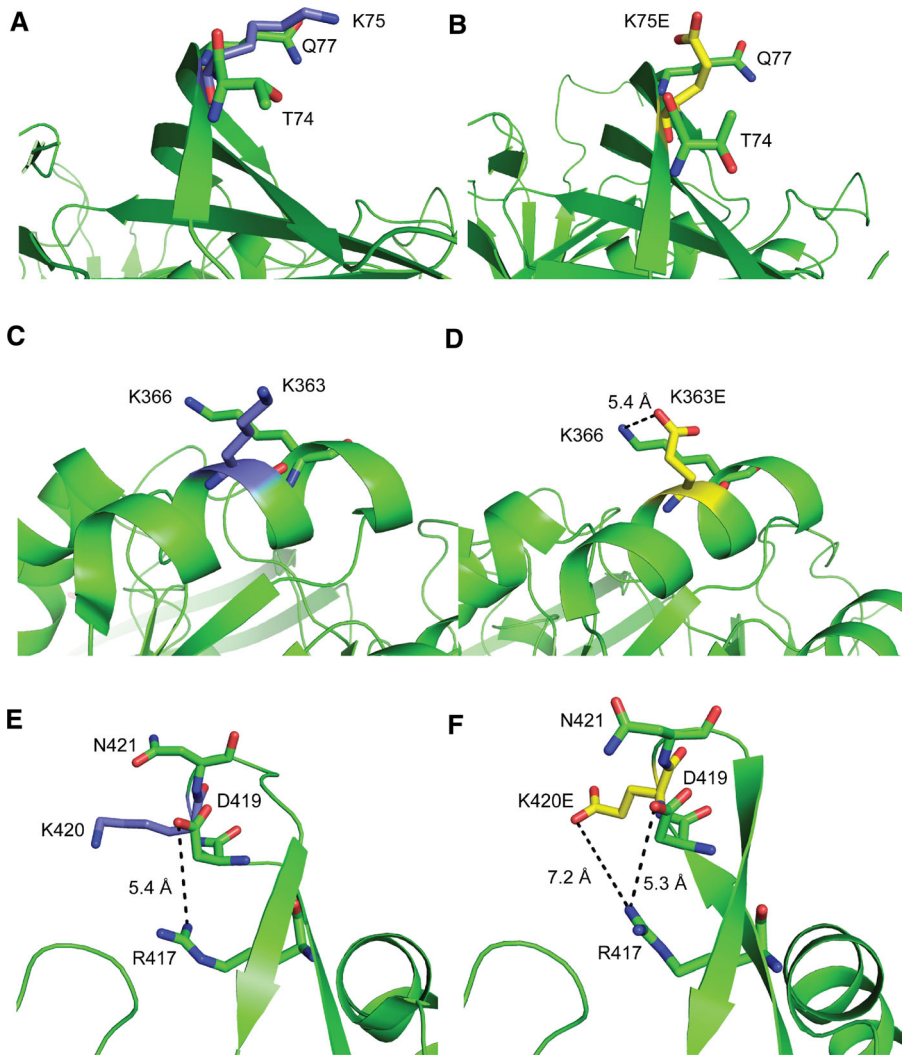

Fig. 5 Close view of the Lys75 (**a**), Lys363 (**c**) and Lys420 (**e**) sites in the crystal structure of PspAG97A and the corresponding sites (**b**, **d**, **f**) in the structural model of its K75E/K363E/K420E mutant

Discussion

In enzyme engineering, it is important to retain the enzyme's activity when manipulating enzyme stability. Some earlier attempts to improve enzyme thermostability have resulted in the reduction of enzyme activity (Guo et al. 2015; Wang et al. 2014). In this study the enzyme stability was increased via optimization of surface charge-charge interactions using the TKSA-MC model (Contessoto et al. 2018), combined with alteration of the enzyme's isoelectric point. Consequently, the mutants generated in this study displayed improved thermostability without compromising the catalytic activity of the WT protein. In addition, earlier studies have shown that beneficial amino acid mutations commonly show additive (Lin et al. 2018) or sometimes asynergistic effect (Wang et al. 2018) on the protein's thermostability. In this study, beneficial amino acid mutations of K75E, K363E and K420E exhibited synergistic effect on the thermostability of the target protein.

The best performing mutant, K75E/K363E/K420E, of the glucodextranase PspAG97A not only shows improved thermostability (remaining 58.8% activity at 35 °C for 90 min compared to the WT remaining 57.8% activity at 35 °C for 20 min), but also retains its

original unique properties, such as high specific activity for dextran (about 1000 U/mg for dextran T5 and 680 U/mg for T70), alkaline-adaption (the optimum pH 7.0–7.5 and retaining more than 80% activity within the range of 7.0–8.0), moderate-temperature catalysis (the optimum temperature 40 °C and retaining more than 80% activity within the range of 35–40 °C) and halophilic (the highest activity at 0.8–1 M NaCl and retaining about 15% activity at physiological 0.15 M NaCl). This thermostability-improved mutant of PspAG97A would be more suitable for application in dental products due to the following reasons. As mentioned before, alkaline oral care products are more protective to enamel than acidic products. However, dextranases reported till now usually function under acidic and mega-thermal conditions (Khalikova et al. 2005). Among them, only a few have been characterized as exo-dextranases (Li et al. 2016; Linder and Sund 1981; Mizuno et al. 1999, 2004; Morimoto et al. 2004; Okazawa et al. 2015; Saburi et al. 2015; Takahashi 1982). To our knowledge, except for PspAG97A (Li et al. 2016) and an isomaltotriose-forming dextranase from *Brevibacterium fuscum* (Mizuno et al. 1999), all reported exo-type dextranases have the optimum pH lower than 7.5. Second, salt (NaCl) has antimicrobial properties (Wijnker et al. 2006) and has been added to some oral care products (Sidhu et al. 2014). Michel et al. evaluated the effectiveness of sea salt-containing mouth rinse and noted a decrease in gingival and periodontal indices at the end of the trial period during which each child rinsed with a solution containing 2.5 g of sea salt in 20 ml of water (Michel et al. 2013). Mani et al. reported a significant reduction in all clinical parameters in 30 adults with gingivitis after mouth rinsing with sea salt for a period compared to those who did not use the rinse (Mani et al. 2015). Therefore, a halophilic dextranase might be better compatible with salt-containing oral care products. Third, this mutant has optimum temperature of 40 °C compared to 35 °C for the WT, and shows improved thermostability within the range of 33.2–38.2 °C in oral temperature (Sund-Levander et al. 2002). Recently, Wang et al. successively reported two alkaline and cold-adapted endo-type dextranases from marine bacteria, suitable for development of dental products (Lai et al. 2019; Ren et al. 2018). In this study, we reported a thermostability-improved alkaline-adapted, mesophilic and halophilic exo-type dextranase from marine bacteria that might have application potential in dental products in combination with alkaline-adapted endo-type dextranases.

In conclusion, the thermostability of an alkaline-adapted, mesophilic and halophilic dextran glucosidase, PspAG97A, was remarkably improved via the optimization of surface charge-charge interaction combined with the shift of the enzyme's pI off its optimum pH value. The best combinational mutant, K75E/K363E/K420E, showed a 7.3-fold increase in the half-life ($t_{1/2}$) at 33 °C compared to that of the WT without compromising the catalytic activity of the WT protein.

Acknowledgements This work was supported by National Natural Science Foundation of China (No. 31570064), and the Key Research Program of the Education Department of Anhui Province (No. KJ2018A0002).

Supporting information Supplementary Figure 1—SDS-PAGE analysis of the recombinant PspAG97A enzyme and its nine single point mutants. M: protein marker; Lane 1–10: PspAG97A, K75E, K135E, K281E, K363E, K366E, K420E, K449E, K595E, K598E

Supplementary Figure 2—Effect of temperature (A–D) and pH (E–H) on enzyme activities of WT PspAG97A and its three thermostability-enhanced single point mutants.

Supplementary Figure 3—SDS-PAGE analysis of the recombinant PspAG97A enzyme and its combinational mutants. M: protein marker; Lane 1–5: PspAG97A, K75E/K363E, K75E/K420E, K363E/K420E, K75E/K363E/K420E.

Supplementary Figure 4—Effect of temperature (A–D) and pH (E–H) on enzyme activities of four thermostability-enhanced multiple point mutants of PspAG97A.

Compliance with ethical standards

Conflict of interest The authors declare no competing financial interest.

References

Contessoto VG, de Oliveira VM, Fernandes BR, Slade GG, Leite VBP (2018) TKSA-MC: a web server for rational mutation through the optimization of protein charge interactions. Proteins 86:1184–1188. https://doi.org/10.1002/prot.25599

Gan W, Zhang H, Zhang Y, Hu X (2014) Biosynthesis of oligodextrans with different Mw by synergistic catalysis of dextransucrase and dextranase. Carbohydr Polym 112:387–395. https://doi.org/10.1016/j.carbpol.2014.06.018

Goulas AK, Cooper JM, Grandison AS, Rastall RA (2004) Synthesis of isomaltooligosaccharides and oligodextrans in a recycle membrane bioreactor by the combined use of dextransucrase and dextranase. Biotechnol Bioeng 88:778–787. https://doi.org/10.1002/bit.20257

Gribenko AV, Patel MM, Liu J, McCallum SA, Wang C, Makhatadze GI (2009) Rational stabilization of enzymes by computational redesign of surface charge-charge interactions. Proc Natl Acad Sci USA 106:2601–2606. https://doi.org/10.1073/pnas.0808220106

Guo J, Rao Z, Yang T, Man Z, Xu M, Zhang X, Yang ST (2015) Enhancement of the thermostability of *Streptomyces kathirae* SC-1 tyrosinase by rational design and empirical mutation. Enzyme Microb Technol 77:54–60. https://doi.org/10.1016/j.enzmictec.2015.06.002

He C et al (2016) Structures of PspAG97A alpha-glucoside hydrolase reveal a novel mechanism for chloride induced activation. J Struct Biol 196:426–436. https://doi.org/10.1016/j.jsb.2016.09.009

Jiménez ER (2009) Dextranase in sugar industry: a review. Sugar Tech 11:124–134. https://doi.org/10.1007/s12355-009-0019-3

Khalikova E, Susi P, Korpela T (2005) Microbial dextran-hydrolyzing enzymes: fundamentals and applications. Microbiol Mol Biol Rev 69:306–325. https://doi.org/10.1128/mmbr.69.2.306-325.2005

Lai X et al (2019) The marine *Catenovulum agarivorans* MNH15 and dextranase: removing dental plaque. Mar Drugs. https://doi.org/10.3390/md17100592

Li W et al (2016) PspAG97A: a halophilic alpha-glucoside hydrolase with wide substrate specificity from glycoside hydrolase family 97. J Microbiol Biotechnol 26:1933–1942. https://doi.org/10.4014/jmb.1606.06047

Lin L, Wang Y, Wu M, Zhu L, Yang L, Lin J (2018) Enhancing the thermostability of fumarase C from *Corynebacterium glutamicum* via molecular modification. Enzyme Microb Technol 115:45–51. https://doi.org/10.1016/j.enzmictec.2018.04.010

Linder L, Sund ML (1981) Characterization of dextran glucosidase (1,6-a-D-glucan glucohydrolase) of *Streptococcus mitis*. Caries Res 15:436–444. https://doi.org/10.1159/000260549

Majeed A, Grobler SR, Moola MH (2011) The pH of various tooth-whitening products on the South African market. Sadj 66:278–281

Makhatadze GI (2017) Linking computation and experiments to study the role of charge–charge interactions in protein folding and stability. Phys Biol 14:013002. https://doi.org/10.1088/1478-3975/14/1/013002

Mani A, Mani S, Anarthe R (2015) A clinical pilot study to evaluate the efficacy of sea salt based oral rinse in gingivitis patients. Int J Exp Dent Sci 4:116–118

Michel JF, Michel MG, Nadan J, Nowzari H (2013) The street children of Manila are affected by early-in-life periodontal infection: description of a treatment modality: sea salt. Refuat Hapeh Vehashinayim (1993) 30(6–13):67

Mizuno T, Mori H, Ito H, Matsui H, Kimura A, Chiba S (1999) Molecular cloning of isomaltotrio-dextranase gene from *Brevibacterium fuscum* var. *dextranlyticum* strain 0407 and its expression in *Escherichia coli*. Biosci Biotechnol Biochem 63:1582–1588. https://doi.org/10.1271/bbb.63.1582

Mizuno M, Tonozuka T, Suzuki S, Uotsu-Tomita R, Kamitori S, Nishikawa A, Sakano Y (2004) Structural insights into substrate specificity and function of glucodextranase. J Biol Chem 279:10575–10583. https://doi.org/10.1074/jbc.M310771200

Morimoto N, Yasukawa Y, Watanabe K, Unno T, Ito H, Matsui H (2004) Cloning and heterologous expression of a glucodextranase gene from *Arthrobacter globiformis* I42, and experimental evidence for the catalytic diad of the recombinant enzyme. J Biosci Bioeng 97:127–130. https://doi.org/10.1016/s1389-1723(04)70179-6

Okazawa Y, Miyazaki T, Yokoi G, Ishizaki Y, Nishikawa A, Tonozuka T (2015) Crystal structure and mutational analysis of isomalto-dextranase, a member of glycoside hydrolase family 27. J Biol Chem 290:26339–26349. https://doi.org/10.1074/jbc.M115.680942

Pleszczynska M, Wiater A, Bachanek T, Szczodrak J (2017) Enzymes in therapy of biofilm-related oral diseases. Biotechnol Appl Biochem 64:337–346. https://doi.org/10.1002/bab.1490

Ren W, Cai R, Yan W, Lyu M, Fang Y, Wang S (2018) Purification and characterization of a biofilm-degradable dextranase from a marine bacterium. Mar Drugs. https://doi.org/10.3390/md16020051

Saburi W, Rachi-Otsuka H, Hondoh H, Okuyama M, Mori H, Kimura A (2015) Structural elements responsible for the glucosidic linkage-selectivity of a glycoside hydrolase family 13 exo-glucosidase. FEBS Lett 589:865–869. https://doi.org/10.1016/j.febslet.2015.02.023

Sidhu P, Kannan S, Muthusamy S, Muthu K (2014) Oral health: bamboo salt. Br Dent J 217:54–54. https://doi.org/10.1038/sj.bdj.2014.601

Sund-Levander M, Forsberg C, Wahren LK (2002) Normal oral, rectal, tympanic and axillary body temperature in adult men and women: a systematic literature review. Scand J Caring Sci 16:122–128. https://doi.org/10.1046/j.1471-6712.2002.00069.x

Takahashi N (1982) Isolation and properties of dextranases from *Bacteroides oralis* Ig4a. Microbiol Immunol 26:375–386. https://doi.org/10.1111/j.1348-0421.1982.tb00188.x

Tu T et al (2015) Improvement in thermostability of an *Achaetomium* sp. strain Xz8 endopolygalacturonase via the optimization of charge-charge interactions. Appl Environ Microbiol 81:6938–6944. https://doi.org/10.1128/aem.01363-15

Wang K et al (2014) Thermostability improvement of a *Streptomyces* xylanase by introducing proline and glutamic acid residues. Appl Environ Microbiol 80:2158–2165. https://doi.org/10.1128/aem.03458-13

Wang Y et al (2018) Increased productivity of L-2-aminobutyric acid and total turnover number of NAD(+)/NADH in a one-pot system through enhanced thermostability of L-threonine deaminase. Biotechnol Lett 40:1551–1559. https://doi.org/10.1007/s10529-018-2607-3

Webb B, Sali A (2016) Comparative protein structure modeling using MODELLER. Curr Protoc Bioinform. https://doi.org/10.1002/cpbi.3

Wijnker JJ, Koop G, Lipman LJ (2006) Antimicrobial properties of salt (NaCl) used for the preservation of natural casings. Food Microbiol 23:657–662. https://doi.org/10.1016/j.fm.2005.11.004

Wu D-T, Zhang H-B, Huang L-J, Hu X-Q (2011) Purification and characterization of extracellular dextranase from a novel producer, *Hypocrea lixii* F1002, and its use in oligodextran production. Process Biochem 46:1942–1950. https://doi.org/10.1016/j.procbio.2011.06.025